Small-Angle Neutron Scattering and Dynamic Light Scattering from a Polyelectrolyte Solution: DNA

Redouane Borsali,† Huy Nguyen, and R. Pecora*

Department of Chemistry, Stanford University, Stanford, California 94305-5080

Received June 24, 1997; Revised Manuscript Received January 7, 1998

ABSTRACT: Static and dynamic properties of a DNA fragment of molecular weight 316 800 (contour length 1632 Å) in semidilute solutions are studied by small-angle neutron scattering (SANS) and static (SLS) and dynamic light scattering (DLS). SANS experiments in a solution with DNA concentration C_p = 42 mg mL^{-1} were performed as functions of added salt concentration C_s and temperature. The resulting plot of scattering intensity $I(q)$ versus scattering wavevector magnitude q shows the existence of a broad peak whose position is independent of both C_s and temperature. Additionally, an "upturn" in the small scattering vector length range (q < 0.01 Å^{-1}) is observed and is temperature-independent. The DLS time correlation function of the same sample shows the two relaxation modes that have previously been observed in DNA and other polyelectrolyte solutions as well as an additional "ultra" slow mode whose corresponding size is much larger than various correlation lengths that may be deduced from SLS experiments and the upturn in the SANS data for small q values.

I. Introduction

Solution properties of polyelectrolytes differ considerably from those of uncharged polymers. The presence of charges along the chain leads to complex intra- and intermolecular interactions that have strong consequences for both the static and dynamic properties of the system. Such interactions can often be screened by adding salt to the solution. The study of these interactions involving polyions, counterions, and co-ions has attracted many researchers, and there has been considerable theoretical[1−11] and experimental[12−25] work in this area over the past decade. Experimental techniques that have been used to probe the behavior of such charged complex systems include static (SLS) and dynamic (DLS) light scattering, small-angle neutron scattering (SANS), small-angle X-ray scattering (SAXS), light microscopy, and more macroscopic techniques such as solution viscometry.

Static scattering experiments in salt-free solutions always show the existence of a maximum at a certain scattering wave vector position, denoted by q*. (It should be recalled that the scattering vector length is given by $q = (4\pi n/\lambda)\sin(\theta/2)$, where λ is the wavelength of the incident beam, θ is the scattering angle, and n is the refractive index of the medium.) It has been shown by several authors that q* scales with the polyelectrolyte concentration as $C_p^{1/2}$ in the semidilute regime and as $C_p^{1/3}$ in the dilute regime. This scattering intensity maximum disappears progressively as salt is added and is, consequently, interpreted to result from long-range electrostatic interactions. These interactions impose a preferential distance between charged particles and lead to an "organized" structure characteristic of a cubic arrangement ($q^* \sim C_p^{1/3}$) in the dilute regime and of a cylindrical or hexagonal packing ($q^* \sim C_p^{1/2}$) in the semidilute domain. We should note that Monte Carlo calculations[26] for rodlike polyelectrolytes using a model potential also lead to this behavior for q*.

† On leave from CERMAV-CNRS and Joseph Fourier University, P.O. Box 53, F-38041, Grenoble Cedex 9, France.

Many theoretical attempts have been made to understand the features of polyelectrolyte systems. These include the use of scaling arguments, which were initiated by de Gennes[2−4] and further developed by Odijk,[6] and the introduction of effective long-range attractive forces by Ise[12] and Odijk.[27,28] There are, however, still no generally accepted interpretations in terms of solution intermolecular structure of the SANS and SAXS scattering peaks and for the upturns in the SANS and SAXS data in the small q range. In this paper both the maximum in the SANS scattering and the low q upturn are investigated as functions of added salt concentration and temperature. Static and dynamic light-scattering experiments are performed to characterize the system and to further elucidate the physical significance of the low q upturn.

II. Experimental Section

II-1. Material and Sample Preparation. High molecular weight calf thymus DNA (Sigma D-1501) was dissolved in 10 M Tris−Cl (pH = 7.8 at 20 °C), 10 M EDTA to a final concentration of 2 mg mL^{-1}. A Heat System XL ultrasonic processor operating at 20 kHz was used to sonicate 5 mL aliquots of this solution at 0 °C for 5 min each. Following sonication, all aliquots were recombined and suspended in TE buffer to 10 mg mL^{-1}. The approximate length of DNA was determined by agarose gel electrophoresis to be ∼400 bp. The gels showed that there at least some fragments ±200 base pairs from the average. Repeated phenol−chloroform extractions were performed to remove any protein from solution. Residual phenol was removed by performing ethyl ether extractions, and the ether was removed in a vacuum. DNA was then ethanol precipitated out of solution and resuspended in doubly distilled water at a concentration of 50 mg mL^{-1}. DNA concentrations were determined by UV absorption at 260 nm. The UV absorbances at 280 nm were also measured to determine the purities of the samples. Any residual NaCl in solution was removed by dialysis of the DNA solution against doubly distilled water. This operation was repeated several times over 4 days (at 4 °C) to ensure a complete "salt-free" system. Doubly distilled water was prepared by redistilling deionized water with a Corning Mega-Pure still. After extensive dialysis, UV absorbance gave a final DNA concentration

S0024-9297(97)00919-4 CCC: $15.00 © 1998 American Chemical Society
Published on Web 02/20/1998

of 42 mg mL^{-1}. The other solutions at different salt concentrations (5, 10, 100, 250, 500, and 1000 mM NaCl) were prepared from the stock "salt-free" system by adjusting the salt content.

II-2. Static and Dynamic Light Scattering. The light-scattering apparatus used in these experiments utilized a Spectra Physics Model 165 argon ion laser operating at 4880 Å. The scattered light from an incident vertically polarized laser beam was measured at different scattering angles in the range 30−130°. This corresponds to a scattering vector length range $0.65 \times 10^{-3} < q$ (Å^{-1}) $< 3.01 \times 10^{-3}$, if the refractive index of the scattering medium $n = 1.33$. Both the static $I(q)$ and dynamic structure factors $S_T(q,t)$ were measured. All static intensities were corrected for the scattering volume variation with angle. The laser power used was between 100 and 500 mW. For dynamic light scattering,[25] autocorrelation functions of the scattered intensity were obtained using a Brookhaven BI9000 autocorrelator. The dynamic structure factor (total intermediate scattering function) $S_T(q,t)$ is related to the measured homodyne intensity autocorrelation function $G^{(2)}(q,t)$ by the Siegert relation:[24,25]

$$G^{(2)}(q,t) = B[1 + \alpha|S_T(q,t)|^2] \quad (1)$$

where B is the baseline and α is the spatial coherence factor dependent upon the scattering geometry and details of the detection system. The constrained regularization method (CONTIN) developed by Provencher[29] was used to obtain the distribution $A(\tau)$ of decay times. A statistical parameter "probability to reject" (P) is calculated for each $A(\tau)$ generated by CONTIN. The preferred solution is usually that with a value of P closest to 0.5.

$$\left[\frac{G^{(2)}(q,t)}{B} - 1\right]^{1/2} = \int_0^\infty A(t)\, e^{-(t/\tau)}\, dt = S_T(q,t) \quad (2)$$

This method, often in concert with the classical technique of fitting to sums of exponentials, is now routinely used to analyze DLS data for polymer systems. It is a powerful method for the determination of the relaxation modes that characterize the system dynamics.

II-3. Small Angle Neutron Scattering. SANS experiments were performed on SANSNG3 at The National Institute of Standards and Technology (NIST, Gaithersburg, MD). The scattering vector length q ranges from 0.0073 to 0.22 Å^{-1}. This was achieved by using two distance sample−detector configurations (2 and 7.5 m). All data obtained were treated according to standard NIST procedures[30] for small angle isotropic scattering (e.g., corrections for transmission and thicknesses of samples). The temperature was controlled to ±1 °C. Despite the high incoherent background scattering from H, the contrast between DNA and D_2O is not as good as that between DNA and H_2O. Therefore, the solvent used in both neutron- and light-scattering experiments was ordinary distilled water (H_2O).

III. Results and Discussion

III-1. Dynamic Light Scattering: Dilute Solution. Dynamic light-scattering experiments were done on dilute solutions of our DNA in order to characterize the sample. Figure 1a shows, for instance, two DLS autocorrelation functions for one dilute and one more concentrated solution at high added salt concentrations. The DNA concentrations are $C_P = 0.07$ mg mL^{-1} (scattering angle $\theta = 90°$) and $C_P = 0.66$ mg mL^{-1} ($\theta = 70°$), and both solutions contain added NaCl at $C_s = 1$ M and are at temperature $T = 20$ °C. (One solution is below the estimated "overlap concentration" $C^* = 0.12$ mg mL^{-1} for this DNA fragment that we deduce below, and the other is above it.) The dots represent the experimental data, and the solid lines, a single exponential fit. The single exponential fit is clearly not satisfactory. A more satisfactory fit was obtained to a sum of two exponentials functions, and the two-exponential fit was confirmed by CONTIN analysis, as shown in Figure 1b. The variations of the frequencies of the two relaxation modes as functions of q^2 are shown in Figure 2. Both the fast and slow modes are, within experimental error, independent of the DNA concentration, and the associated diffusion coefficients determined at low q ($D = (\Gamma/q^2)_{q\to 0}$) are $D_F = 1.34 \times 10^{-7}$ cm^2 s^{-1} and $D_S = 2.57 \times 10^{-8}$ cm^2 s^{-1}.

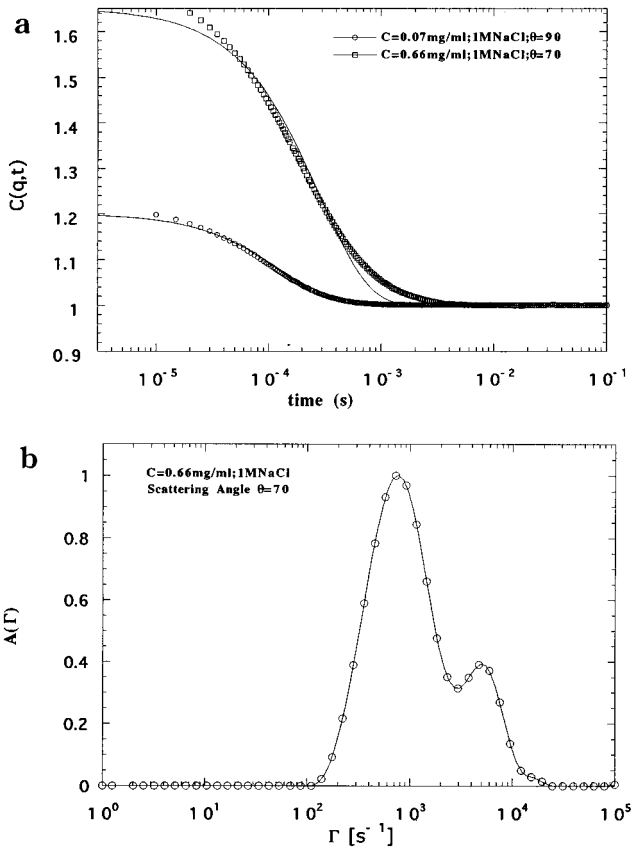

Figure 1. (a) DLS: Typical autocorrelation function as measured by DLS on the DNA in "salt-free" and 1 M NaCl solutions for $C_p = 0.07$ mg mL^{-1} ($\theta = 90°$) and $C_p = 0.66$ mg mL^{-1} ($\theta = 70°$). The dots represent the experimental data, and the solid line is a single-exponential fit. (b) DLS, CONTIN analysis. Same system as Figure 1a.

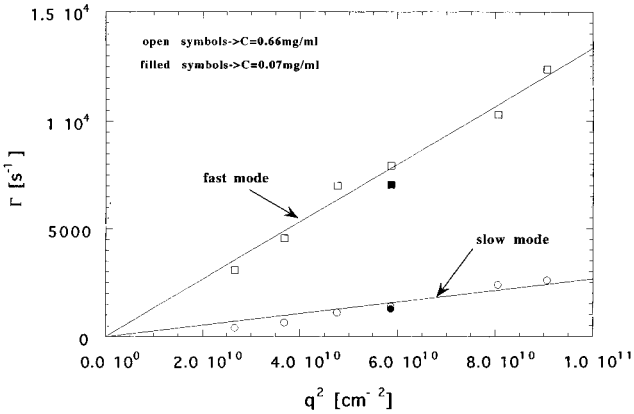

Figure 2. DLS: Variation of the frequencies of the fast and slow relaxation modes as a function of q^2 for the concentrations shown.

The fast mode is interpreted as in previous work on DNA[31−36] as arising from the dynamics of concentration

fluctuations (cooperative mode) of monomeric DNA. Its extrapolation to infinite dilution would give the translational self-diffusion coefficient of single DNA molecules. The hydrodynamic radius obtained from the Stokes−Einstein relation for this mode at the concentrations studied is $R_h = 159.6$ Å.

It is possible to calculate the contour length L of the DNA from the translational diffusion coefficient of the molecule provided the diameter of the DNA helix and its persistence length are known. For a perfectly rigid rod ($L \ll P$), the Broersma[37] relation may be used

$$D = \frac{k_B T}{3\pi\eta_o L}\left[\ln(2p) + \frac{1}{2}(\gamma_{\parallel} + \gamma_{\perp})\right] \quad (3)$$

where

$$\gamma_{\parallel} = -0.193 + \frac{0.15}{\ln(2p)} + \frac{8.1}{\ln^2(2p)} - \frac{18}{\ln^3(2p)} + \frac{9}{\ln^4(2p)} \quad (4)$$

$$\gamma_{\perp} = 0.807 + \frac{0.15}{\ln(2p)} + \frac{13.5}{\ln^2(2p)} - \frac{37}{\ln^3(2p)} + \frac{22}{\ln^4(2p)} \quad (5)$$

An alternative formula for the rigid rod translational diffusion coefficient has been given by Tirado and Garcia de la Torre[38]

$$D = \frac{k_B T}{3\pi\eta_o L}(\ln p + \nu) \qquad \text{where} \qquad \nu = 0.312 + \frac{0.565}{p} - \frac{0.1}{p^2} \quad (6)$$

In these relations $k_B T$ is the Boltzmann energy, $p = (L/d)$ is the ratio of the length to the cross section diameter, and η_o is the viscosity of the solvent. The hydrodynamic diameter of DNA has been determined by Eimer and Pecora[39] to be 20.5 Å. Our SANS experiments at high q values (see below) show that 2 times the cross-section radius of gyration of DNA is about $d = 20.1$ Å. Using this value for d, the above relations give $L = 1396$ Å (Broersma) and $L = 1432$ Å (Tirado−Garcia de la Torre). The validity of the Tirado−Garcia de la Torre relation is estimated to be in the p range $5 < p < 30$. Both relations indicate that p is about 70 for our DNA.

The DNA of the contour lengths given above is a semiflexible molecule and deviations from rigid rod shape should affect the diffusion coefficient. The hydrodynamic model developed for wormlike chains by Yamakawa and Fuji[40] gives an expression for the translational diffusion coefficient of a semiflexible coil as a function of the persistence length, the contour length, and the molecular diameter. Sorlie and Pecora[41] have shown that this model gives good agreement with the diffusion coefficients measured in their DLS experiments on DNA restriction fragments in the range from 360 to 2311 base pairs. We reverse this procedure in our case and use the measured diffusion coefficient to obtain the contour length. For DNA in high salt content the consensus persistence length is $L_p = 500$ Å. We use this value, the measured diffusion coefficient and the DNA diameter given above, and the Yamakawa−Fuji relation to obtain a contour length $L = 1632$ Å. This contour length is, of course, larger than that determined from the rigid rod relations.

The radius of gyration of a wormlike chain may be found from the Benoit−Doty relation[42]

$$R_g^2 = \frac{LL_p}{3} - L_p^2 + \frac{2L_p^3}{L} - \frac{2L_p^4}{L^2}\left(1 - \exp\left[-\frac{L}{L_p}\right]\right) \quad (7)$$

Using the consensus persistence length in high salt content and the value of the contour length determined above, we find that $R_g = 360.6$ Å. Furthermore, using the hydrodynamic radius determined from the DLS fast mode, the ratio of the radius of gyration to the hydrodynamic radius, $R_g/R_h = 2.26$.

An estimate of the "overlap" concentration C^* at low salt content may be calculated from the contour length L, and molecular weight M_w of the DNA and Avogadro's number N_A:

$$C^* = M_w/N_A L^3$$

This relation is appropriate for rigid rod macromolecules. It defines the onset concentration at which there is an average of one rod in the volume L^3. Using the contour length $L = 1632$ Å deduced above from our DLS measurements, we find $C^* = 0.12$ mg mL^{-1}. For solutions with added salt, the molecule should be more flexible than in low or no added salt solutions and L would then be an effective length that is shorter than the contour length.

The slow mode has been the subject of much interest and controversy in the past decade. It has been observed in a variety of synthetic and biological polymers, including DNA.[31−36] The hydrodynamic radius associated with this slow mode is $R_h = 835$ Å in 1 M NaCl for our DNA at concentrations up to $C_P = 0.66$ mg mL^{-1}. It is the same size, about 1000 Å, as found for other DNAs as well as other polyelectrolytes under "salt-free" conditions. Several interpretations of the slow mode have been given: The most common is that it is due to scattering from aggregates or clusters formed by multipolymer chain domains. Whether these domains are stable or temporal (due to incomplete solubility), "filterable" or not, has been a subject of much discussion.[43,44] In this work, among other things, we confirm the existence of this slow mode, already observed for DNAs under various solution conditions.[31−36] We would like to mention also that this slow mode was in fact observed for our DNA even at relatively low DNA concentrations. A slow mode has also been observed at low concentrations for a 20 base pair oligonucleotide.[36] We do not speculate further on the physical meaning of this slow mode, since the literature is already abundant with possible explanations.

To further elucidate the dynamical behavior of the DNA solutions, we investigated SLS and DLS from our DNA system at higher concentrations. In particular we performed SLS and DLS experiments on the same solutions where an upturn of the scattered intensity in the small q range was observed in our SANS experiments (see section III-2.2). If there is a long-range multichain correlation, we expect that it may be seen at low q in the SANS, at even lower q in the SLS, and also as one or more slow modes in the DLS.

III-2.1. SANS: Effect of Salt Concentration. Figure 3 shows the variation of the SANS scattering intensity $I(q)$ as a function of q at different added salt concentrations C_s. The added salt concentrations are $C_s = 0$ ("salt-free"), 10 mM, 50 mM, 0.5 M, and 1 M). In

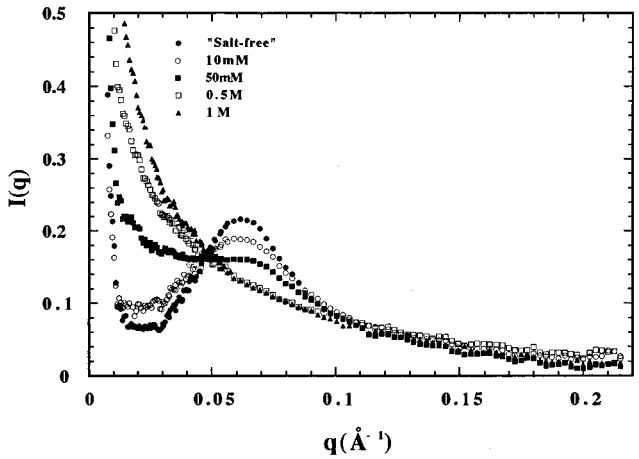

Figure 3. SANS: Effect of added salt. Variation of $I(q)$ as a function of q for ($M_w = 2.92 \times 10^5$, $C_p = 42$ mg mL^{-1}) DNA at different added salt concentrations, C_s.

the "salt-free" case and for our $C_p = 42$ mg mL^{-1}, a very distinct and broad peak with an upturn in the small q range is observed. The position of such a peak is often correlated with the main peak in the radial distribution function for the polymer segments at a radial distance approximately equal to $2\pi/q^*$. Because of this correspondence, we shall call $d^* \equiv 2\pi/q^*$ the "Bragg distance" below.

Although the DNA for this molecular weight is not expected to be in the rigid rod limit, the position of the maximum is in good agreement with a model of local cylindrical or hexagonal order rather than one with a uniform distribution. The variation of the peak position, under salt-free conditions, is given as a function of polyelectrolyte concentration assuming a cylindrical distribution of the molecules by

$$q^* = 2\pi\left[\frac{\pi C_p\ (\text{g/cm}^3)\ N_A}{4M_L}\right]^{1/2} \qquad (8)$$

where $M_L = 194.11$ (M_L = m/L is the mass per unit length; $m = 660$ and $l = 3.4$ Å).

Similar theoretical variations of q^* are given for hexagonal packing, $q^* = 2\pi[\sin 60°\ C_p\ (\text{g/cm}^3)\ N_A/M_L]^{1/2}$, and for a uniform distribution, $q^* = 2\pi[C_P\ (\text{g/cm}^3)\ N_A/M_w]^{1/3}$, for comparison. From our peak position data and those reported by Wang and Bloomfield[15] for a DNA sample with contour $L = 500$ Å, we find that the uniform distribution is unsatisfactory. Although the difference between the cylindrical and hexagonal packings is not very large, the data seem to agree best with the cylindrical local order. It is worth noting from a comparison of our results with those of Wang and Bloomfield that the peak position is independent of the molecular weight in the semidilute range of concentration. In our experiments, one observes that the addition of a simple electrolyte (NaCl) decreases the peak intensity and maintains its position roughly constant. When enough salt is added, the scattering behavior is closer to that of a neutral polymer. For example, this neutral type behavior is reached for $C_p = 42$ mg mL^{-1} at values of C_s above about 300 mM NaCl. This behavior is a reflection of the electrostatic nature of the peak. A progressive screening of electrostatic forces is observed when C_s increases and neutral behavior is eventually recovered. All these features, except the constancy of the peak position upon adding salt, have been reported by several other authors[3,12,14,16,21–23] with, however, differing interpretations, as we discuss below.

It is worth noting that the equivalent interparticle distance (the Bragg distance obtained from the peak position, $d^* = 2\pi/q^*$) does not change with ionic strength in our experiments. For this DNA system at concentration $C_p = 42$ mg mL^{-1}, where $q^* = 0.062$ Å^{-1}, the Bragg distance corresponds to $d = 101.3$ Å. On the other hand, for $q < q^*$, the scattering intensity is very sensitive to the addition of salt and for $q > q^*$, $I(q)$ preserves a level of scattering close to the value in the absence of salt as expected by most theoretical models for electrostatic interactions in the semidilute range of concentration. It is finally interesting to note that there is a sort of "isobestic" point located at roughly $q = 0.05$ Å^{-1} ($d = 125.7$ Å) where all the intensities are independent of the salt concentration. So far no theoretical model has been formulated to explain this observation, although it is common to several different polyelectrolyte systems.[17,21]

Our results differ from those reported by Wang and Bloomfield[15] in two respects. One is the effect of salt on the peak position discussed above and the other concerns the behavior of the intensity at small q values ($q < 0.02$ Å^{-1}). The effect of salt is very different from that reported by Wang and Bloomfield[15] when using SAXS on their DNA system at $C_p = 72$ mg mL^{-1}. Their results show a peak position that is strongly dependent on the added salt concentration. The interpretation given for this dependence is that a transition from hexagonal packing to a uniform distribution of the DNA molecules occurs as salt is added. The only difference between the Wang and Bloomfield[15] system and the one used in the present work is the DNA contour length. Indeed, in our system the DNA contour length is about 1632 Å, whereas in ref 15 it is about 500 Å, which is also approximately the persistence length at high salt. We do not have any explanation for why the peak position should depend on the added salt concentration for persistence length DNA molecules and be independent of salt for longer lengths. More recent SAXS experiments on relatively dilute solutions of 150 and 22 000 base pair DNA,[45] (DNA concentration ranging from 2 to 10 mg mL^{-1}) shows that there is little change in the position of the maximum of the scattering intensity with added salt concentration. In fact, q^* goes to slightly higher values as the salt content is increased, which is in the opposite direction from the Wang and Bloomfield[15] results. The effect of salt on the peak position is still not very well understood. Different systems, and sometimes even similar systems, show different behaviors leading to different interpretations and speculations.

III-2.2. SANS: Upturn and Asymptotic Behavior. Although the low q upturn has been observed in many polyelectrolyte experiments, there is still a lack of understanding of its physical meaning. As has been discussed above, the upturn is clearly observed in our experiments (see Figure 3), whereas it was not reported in the SAXS experiments of Wang and Bloomfield.[15] This may be due to the geometry of the X-ray apparatus limiting the range of angles that could be studied. Data at angles corresponding to q below 0.03 Å^{-1} were not reported, and the upturn could appear in this region for their sample. The physical interpretation of the upturn still constitutes a challenging problem. One way

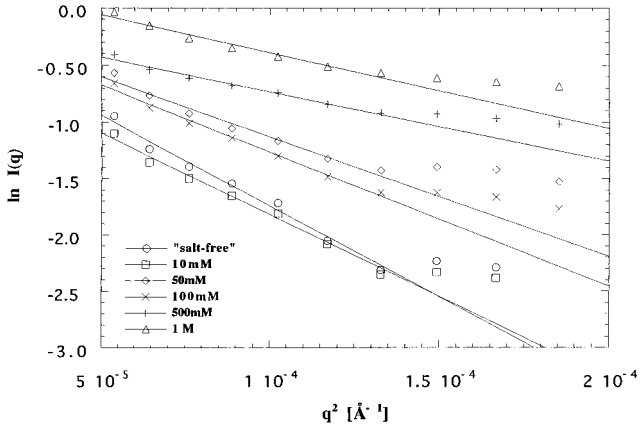

Figure 4. SANS: Variation of ln $I(q)$, in the Guinier approximation, versus q^2.

of addressing this problem[46] is to analyze the data in terms of Guinier methods. At small angles, the scattering intensity can be approximated by the Guinier equation, yielding an overall apparent radius of gyration $R_{g,upturn}$

$$\ln I(q) = \ln I_0 - q^2 R_{g,upturn}{}^2/3 \qquad (9)$$

Strictly speaking, Guinier techniques apply only to dilute solutions. Our point of view, however, is that this apparent radius of gyration could correspond to a dilute aggregate or it could simply be a correlation length giving the scale of a (dilute) local inhomogeneity. We have analyzed our data within this framework for different salt concentrations. This is illustrated in Figure 4 where ln $I(q)$ is plotted against q^2 and where only the linear part of the scattering data has been taken into account for the analysis. The results of the fit are listed in Table 1. The apparent radius of gyration decreases from 219 to 135 Å when the added salt content increases from "salt-free" to 1 M. These values are too small to be compared to the size of even single chain DNA (R_g = 361 Å) at infinite dilution.

We give an argument similar to that given by Matsuoka, Schwann, and Ise[46] in analyzing the SANS upturn region of aqueous solutions of sodium poly(styrenesulfonate). They argue that the apparent R_g is due to a cluster of chains packed a distance d^* apart. We calculate the radius $R = (5/3)^{1/2}R_g$ corresponding to this radius of gyration and then estimate how many cylinders of length $2R$ can be packed in a spherical volume corresponding to this radius if they are d^* apart. The volume allocated to one cylinder is $V_{chain} = \pi(d^*/2)^2 2R$. The number N of chains in each cluster is then approximated by $N = (4/3)\pi R^3/V_{chain}$. The results of this rather rough analysis are given in Table 1. The results show that N estimated in this way varies from about 21 cylinders of length $2R$ (parts of DNA molecules) in the "salt-free" solution to about 5 at 1 M NaCl. As we discuss below, however, static and dynamic light-scattering experiments indicate that the neutron q domain investigated does not attain q small enough to extract an overall correlation length that can be identified as the whole size of the scattering domain.

We have also analyzed the asymptotic behavior at large q values ($I \sim q^\alpha$). In excess of salt (C_s = 1 M NaCl), we obtain $\alpha = -1$, which is in perfect agreement with the value we expect for a rigid rod. Indeed, at this scale of q the DNA is rigid and independent of molecular

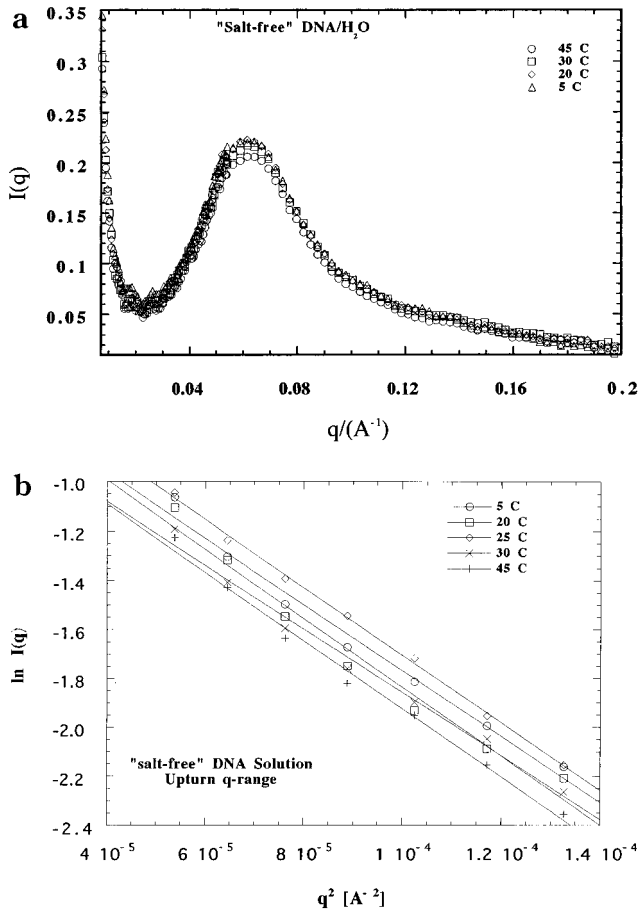

Figure 5. (a) SANS: Effect of temperature. Variation of $I(q)$ versus q for salt-free solutions at the various temperatures shown (region of the maximum). (b) SANS: Effect of temperature. Variation of $I(q)$ versus q^2 for salt-free solutions at the various temperatures shown (region of the upturn).

Table 1. Characteristic Sizes, SANS Upturn Domain

	C_s = 0	C_s = 10 mM	C_s = 50 mM	C_s = 0.1 M	C_s = 0.5 M	C_s = 1 M
R_g (Å), upturn	219	208	189	178	141	135
R (Å) (sphere)	282	268	244	229	182	174
N^a	20.6	18.6	15.5	13.6	8.6	4.7

[a] N is calculated as described in the text using d^* = 101.3 Å.

weight. For the "salt-free" solution or for low ionic strengths (e.g., up to C_s = 300 mM NaCl), the analysis of the asymptotic behavior for $q > q^*$ gives, however, an exponent α very close to -2. To our knowledge, such an analysis has never been done before and the value of the exponent would suggest a locally Gaussian distribution of DNA segments.

The asymptotic behavior of $I(q)$ at high q may be used to determine the cross-sectional diameter R_c of the DNA chain. We use the expression for the scattered intensity at very high q for a molecule that is assumed to be rigid and cylindrically shaped,[47]

$$I(q) = I_0 e^{-q^2 R^2 c/2} \qquad (10)$$

From the slope of our plot, we obtain an estimate for the cross-sectional radius of gyration for the DNA R_c = 10.05 Å. This radius, within experimental error, is found to be independent of salt concentration. This is in excellent agreement with the R_c determined by SAXS studies of short and long DNA in dilute solution in the

presence of NaCl.[45,48,49] This radius is also comparable to the hydrodynamic radius of DNA, 10.5 Å, determined by measurements of translational and rotational diffusion coefficients of oligonucleotides in dilute solution by Eimer and Pecora.[39]

III-3. SANS: Effect of Temperature. It is worth noting that some polyelectrolytes may undergo a phase transition to a mesophase.[4,50−53] This often occurs as the temperature changes or when the charge density decreases, resulting in a decrease in the quality of the solvent. For our DNA sample, the shape of the SANS result, namely $I(q)$ versus q, is not very sensitive to temperature changes over the range 5−45 °C. This is not surprising since DNA belongs to the class of highly charged and relatively rigid polyions. This behavior is illustrated in Figure 5a. There is a slight broadening of the maximum and a decrease in peak height with increasing temperature. This is consistent with the slight increase of thermal motion. The same observation has been made on other systems.[54] On the other hand, the values of $I(q)$ in the upturn area are sensitive to the temperature, as shown in Figure 5b. However, as may be seen from the slopes, the size associated with the upturn does not change with temperature

III-4. Static and Dynamic Light Scattering: Upturn Domain. Two solutions were chosen to investigate the upturn and its relation with the corresponding characteristic size revealed by static and dynamic light-scattering experiments. The light-scattering experiments were performed on the same solutions used for SANS, namely $C = 42$ mg mL^{-1}: "salt-free" and 1 M NaCl. The SLS intensity as a function of q, $I(q)$, is plotted in Figure 6a. One observes that $I(q)$ increases sharply as q decreases. This behavior indicates the existence of large size aggregates (or a large correlation length). This is illustrated in Figure 6b where ln $I(q)$ is plotted as a function of q^2, yielding "apparent" radii of gyration of about 1400 Å for $C_s = 1$ M NaCl and 1490 Å for the "salt-free" solution. These values are very large compared to those extracted from the low angle upturn in the SANS experiments (see Table 1). It is clear that the neutron experiments did not attain low enough q values to give an overall size.

Typical DLS intensity autocorrelation functions at a scattering angle $\theta = 90°$ and $T = 25$ °C are displayed in Figure 7a for both salt-free and 1 M NaCl solutions. Obviously, a single-exponential cannot describe the autocorrelation functions. Analysis of the data with CONTIN and multiexponential fits shows that the autocorrelation functions are best described by three relaxation modes (see Figure 7b). In 1 M NaCl, the fast mode $D = 1.33 \times 10^{-7}$ cm^2 s^{-1} is identified with the fast mode measured for very dilute solutions. Within experimental error, it is found that the fast mode does not change with DNA concentration. The second mode for the "salt-free" solution ($D = 6.5 \times 10^{-10}$ cm^2 s^{-1}) and that for 1 M NaCl ($D = 7.47 \times 10^{-10}$ cm^2 s^{-1}) correspond, we believe, to the slow modes measured in more dilute solutions. The diffusion coefficients of these modes usually decrease with increasing DNA concentration, in contrast to the fast mode, which is observed in this case to be essentially constant. The physical meaning attributed to these two relaxation modes, found also in other systems, has recently been addressed extensively by Sedlak.[44]

In both of our nondilute solutions, however, the main contribution to the dynamics (amplitude about 70% of the total amplitude) comes from an "ultra" slow mode ($D = 3.56 \times 10^{-12}$ cm^2/s for "salt-free"; $D = 1.71 \times 10^{-12}$ cm^2/s for 1 M NaCl solution). Similar observations on concentrated DNA solutions have been made by Wissenburg et al.[27] They observed ultra slow modes in DLS experiments on 160 base pair DNA fragments above a certain critical concentration that increases with increasing added salt concentration. These authors, in addition to dynamic light scattering, have also performed cryoelectron microscopy experiments. In the solutions in which ultra slow modes are observed in the dynamic light scattering, what appear to be loose aggregates of DNA globules are observed in the electron micrographs.

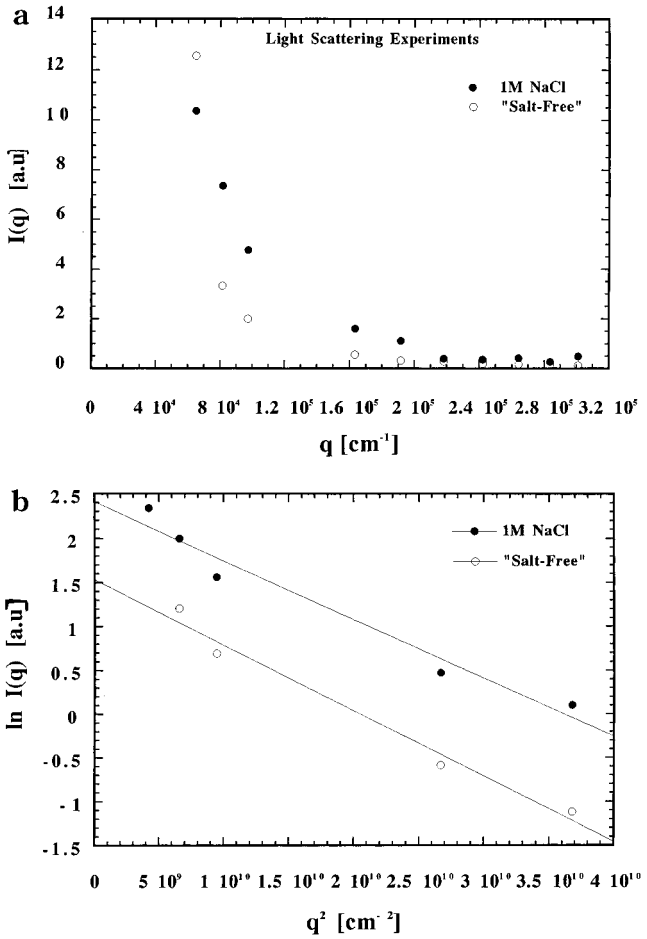

Figure 6. (a) Static light scattering: Variation of $I(q)$ versus q for salt-free and 1 M NaCl solutions (b) Static light scattering: Variation of ln $I(q)$ versus q^2 for salt-free and 1 M NaCl solutions.

IV. Conclusion

In this paper we have investigated the structure and dynamics of DNA solutions in the dilute and semidilute range of concentrations at different temperatures with and without added salt using small angle neutron scattering and static and dynamic light scattering. The SANS results in the semidilute solutions show the existence of a single, pronounced peak in the scattered intensity whose position scales with the DNA concentration as $q^* \sim C_p^{1/2}$ and remains unchanged for different ionic concentrations and temperature. This latter result on the lack of a salt effect on the peak position contrasts with that from SAXS observations by Wang and Bloomfield[15] on persistence length DNA.

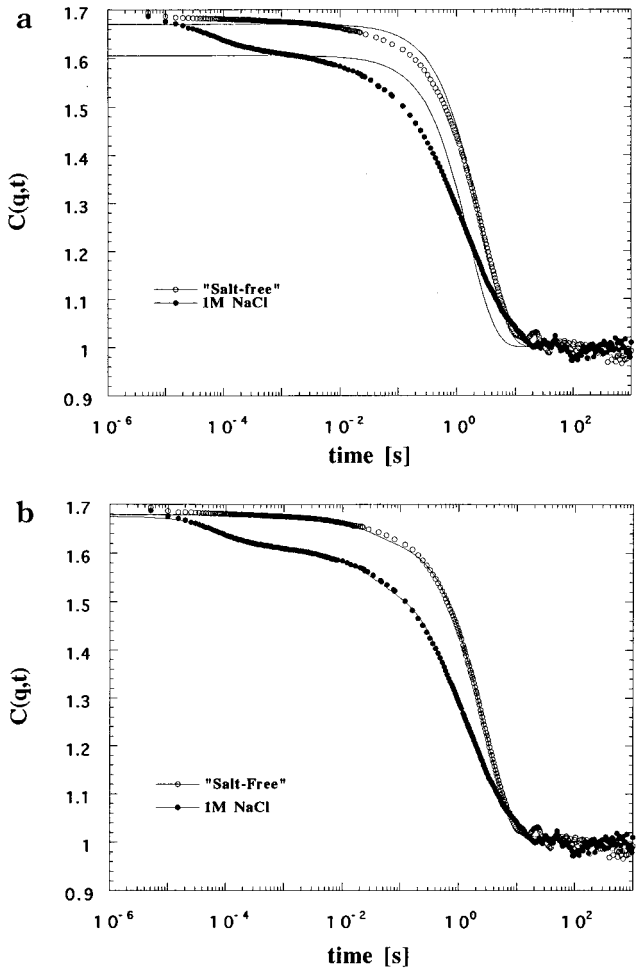

Figure 7. (a) DLS: Typical DLS autocorrelation functions for the DNA "salt-free" and 1 M NaCl solutions for $C_p = 42$ mg mL^{-1} ($\theta = 90°$). The dots represent the experimental data, and the solid line is a single-exponential fit. (b) DLS: Same system as Figure 7a with a three-exponential fit.

In addition to the peak discussed above, there is a distinct upturn of scattered SANS intensity in the very small q range (typically, $q < 0.02$ Å^{-1}) for all studied samples. Similar behavior has been observed in the SANS data in other systems, for instance, flexible polyelectrolytes (PSSNa)[14] and polysaccharides.[21] The region of this upturn was studied also by means of static light scattering, and the results show that the overall size values are very large compared to those extracted from the low angle upturn in the SANS experiments and suggest that caution has to be taken in extracting "sizes" from the very low angle SANS data.

Finally, the DLS experiments performed at different DNA and added salt concentrations show that in addition to the well-documented two modes (cooperative and slow), there is an "ultra slow mode", suggesting the existence of large aggregates. These aggregates have been directly observed by other authors[28] using cryo-electron microscopy.

Acknowledgment. The authors are grateful to Dr. Boualem Hammouda for his very kind assistance in the SANS experiments and Edward Hanson for his help with the DLS. This work was supported by National Science Foundation Grant No. CHE-9520845 and the NSF-MSERC program at Stanford University. We acknowledge the support of the National Institute of Standards and Technology, United States, Department of Commerce, in providing the neutron research facilities used in this experiment. This work is also based upon activities supported by the National Science Foundation under Agreement No. DMR-9423101.

References and Notes

(1) Katchalsky, A.; Alexandrowicz, Z.; Kedem, O. In *Chemical Physics of Ionic Solutions*; Conway, Barradas, Eds.; Wiley: NY, 1976.
(2) de Gennes, P.-G. *Scaling Concepts in Polymer Physics*; Cornell University Press: Ithaca, NY, 1979.
(3) Hayter, J.; Jannink, G.; Brochard F.; de Gennes P.-G. *J. Phys. Lett. (Paris)* **1980**, *41*, L-451.
(4) de Gennes, P.-G.; Pincus, P.; Velasco, R. M.; Brochard F. *J. Phys. (Paris)* **1976**, *37*, 1461.
(5) Benmouna, M.; Weill G.; Benoit, H.; Akcasu, A. Z. *J. Phys. (Paris)* **1982**, *43*, 1679.
(6) Odijk, T. *J. Polym. Sci., Polym. Phys. Ed.* **1977**, *15*, 477.
(7) Skolnick, J.; Fixman, M. *Macromolecules* **1977**, *10*, 9444.
(8) Le Bret, M. *J. Chem. Phys.* **1982**, *76*, 6273.
(9) Manning, G. S. *Rev. Biophys.* **1978**, *11*, 179.
(10) Hess, W.; Klein, R. *Adv. Polym. Sci.* **1982**, *32*, 173.
(11) Vilgis, T.; Borsali, R. *Phys. Rev. A* **1991**, *43*, 6857.
(12) Ise, N. *Angew. Chem., Int. Ed. Engl.* **1986**, *25*, 323.
(13) Kaji, K.; Urakawa, H.; Kanaya, T.; Kitamaru, R. *J. Phys. (Paris)* **1988**, *49*, 993.
(14) Nierlich, M.; et al. *J. Phys. (Paris)* **1979**, *40*, 701.
(15) Wang, L.; Bloomfield, V. *Macromolecules* **1991**, *24*, 5791.
(16) Drifford, M.; Dalbiez, J. P. *J. Phys. Chem.* **1984**, *88*, 5368.
(17) Xiao, L.; Reed, W. F. *J. Chem. Phys.* **1991**, *94*, 4568.
(18) Ghosh S.; Peitzsch, R. M.; Reed, W. F. *Biopolymers* **1992**, *32*, 1105.
(19) Lin, S. C.; Lee, W. I.; Schurr, M. J. *Biopolymers* **1978**, *17*, 1041.
(20) Sedlak, M.; Amis, E. *J. Chem. Phys.* **1992**, *96*, 817.
(21) Morfin, I.; Reed, W.; Rinaudo, M.; Borsali, R. *J. Phys. II* **1994**, *4*, 1001.
(22) Forster, S.; Schmidt, M.; Antonietti, M. *Polymer* **1990**, *31*, 781.
(23) Maier, E. E.; Krause, R.; Deggelmann, M.; Hagenbtchle, M.; Weber, R.; Fraden, S. *Macromolecules* **1992**, *25*, 1125.
(24) Schmitz, K. *Dynamic Light Scattering by Macromolecules*; Academic Press: New York, 1990; Chapter 10.
(25) Berne, B. J.; Pecora, R. *Dynamic Light Scattering with Applications to Chemistry, Biology and Physics*; Wiley: New York, 1976.
(26) Weyerich, B.; D'Aguanno, B.; Canessa, E.; Klein, R. *Faraday Discuss. Chem. Soc.* **1990**, *90*, 245.
(27) Odijk, T. *Macromolecules* **1994**, *27*, 4998.
(28) Wissenburg, P.; Odijk, T.; Cirkel, P.; Mandel, M. *Macromolecules* **1995**, *28*, 2315.
(29) Provencher, S. W.; Hendrix, J.; Maeyer, L. De; Paulussen N. *J. Chem. Phys.* **1978**, *69*, 4273. Provencher, S. W *Comput. Phys. Commun.* **1982**, *27*, 213, 229.
(30) SANS Data Reduction and Imaging Software. National Institute of Standards and Technology Center for Neutron Research, September 1997. Available at the NIST Internet site: http://www.nist.gov/.
(31) Nicolai, T.; Mandel, M. *Macromolecules* **1989**, *22*, 438.
(32) Goinga, H. Tj.; Pecora, R. *Macromolecules* **1991**, *24*, 6128.
(33) Ferrari, M. E.; Bloomfield, V. A. *Macromolecules* **1992**, *25*, 5266.
(34) Newman, J.; Tracy, J.; Pecora, R. *Macromolecules* **1994**, *27*, 6808.
(35) Seils, J.; Pecora, R. *Macromolecules* **1995**, *28*, 661.
(36) Liu, H. Ph.D. Thesis, Stanford University, 1996.
(37) Broersma, S. *J. Chem. Phys.* **1960**, *32*, 1626; 1632; **1981**, *74*, 6989.
(38) Tirado, M.; Garcia de la Torre, J. *J. Chem Phys.* **1979**, *71*, 2581; **1980**, *73*, 1986.
(39) Eimer, W.; Pecora, R. *J. Chem. Phys.* **1991**, *94*, 2324.
(40) Yamakawa, H.; Fujii, M. *Macromolecules* **1973**, *6*, 407.
(41) Sorlie, S. S.; Pecora, R. *Macromolecules* **1990**, *23*, 487.
(42) Benoit, H.; Doty, P. *J. Chem. Phys.* **1953**, *57*, 958.
(43) Reed, W. *Macromolecules* **1994**, *27*, 873.
(44) Sedlak, M. *J. Chem. Phys.* **1996**, *105*, 10123.
(45) Koch, M. H. J.; Sayers, Z.; Sicre, P.; Svergun, D. *Macromolecules* **1995**, *28*, 4904.
(46) Matsuoka, H.; Schwahn, D.; Ise, N. *Macromolecules* **1991**, *24*, 4227.

(47) Porod, G. *Acta Phys. Aust.* **1948**, *2*, 255. Kratky, O.; Porod, G. *Ibid.* **1948**, *2*, 133.
(48) Luzzati, V.; Masson, F.; Mathis, A.; Saludjian, P. *Biopolymers* **1976**, *4*, 491.
(49) Garcia de la Torre, J.; Horta, A. *J. Phys. Chem.* **1976**, *80*, 2028.
(50) Khokhlov. A. *J. Phys. A: Math. Gen.* **1980**, *13*, 979.
(51) Khokhlov, A.; Khachaturian, K. *Polymer* **1982**, *23*, 1742.
(52) Borue, V.; Eurokomovich, X. *Macromolecules* **1988**, *21*, 3240.
(53) Joanny, J. F.; Leibler, L. *J. Phys.* **1990**, *51*, 545.
(54) Boue, F.; Cotton, J. P.; Lapp, A.; Jannink, G. *J. Chem. Phys.* **1994**, *101*, 2562.

MA970919B